

13. M. L. Mayer, G. L. Westbrook, P. B. Guthrie, *Nature* **309**, 261 (1984).
14. G. Stuart, N. Spruston, B. Sakmann, M. Häusser, *Trends Neurosci.* **20**, 125 (1997).
15. P. Fatt, *J. Neurophysiol.* **20**, 61 (1957).
16. These experiments were performed in the presence of ZD7288 (10 μ M; Tocris, Bristol, UK) to block the effect of the hyperpolarization-activated current I_h on somatic EPSP time course (22). APs in these experiments were evoked 5 ms after EPSP onset. In control conditions, there was a smaller but still significant difference between shunting of EPSPs generated at distal (>200 μ m) and at more proximal locations ($34 \pm 5\%$ versus $22 \pm 2\%$ of control; $n = 10$; $P < 0.05$).
17. The EPSP shunting was measured before and after application of TTX (1 μ M) to the dendritic recording site using a puffer pipette. Somatic AP amplitude was unaffected by these applications of TTX ($-4 \pm 4\%$ change; $P > 0.05$). APs in these experiments were evoked by brief somatic current injections 6 to 7 ms after dendritic EPSP onset.
18. Simulations were performed using NEURON (23) with a time step of 10 μ s. The single-compartment model consisted of a cylinder 10 μ m long and 10 μ m in diameter, with $C_m = 1 \mu$ F/cm², $R_m = 12$ k Ω cm² and a passive reversal potential of -65 mV. The synaptic conductance (5 pS) had a reversal potential of 0 mV and exponential rise and decay kinetics, with $\tau_{rise} = 0.3$ ms and $\tau_{decay} = 3$ ms.
19. Supplemental Web material is available on Science Online at www.sciencemag.org/cgi/content/full/291/5501/138/DC1.
20. D. M. Armstrong, J. A. Rawson, *J. Physiol. (London)* **289**, 425 (1979).
21. G. J. Stuart, H. U. Dodt, B. Sakmann, *Pfluegers Arch.* **423**, 511 (1993).
22. S. R. Williams, G. J. Stuart, *J. Neurophysiol.* **83**, 3177 (2000).
23. M. L. Hines, N. T. Carnevale, *Neural Comput.* **9**, 1179 (1997).
24. M.H. and G.J.S. performed the experiments, analysis, and simulations; G.M. carried out preliminary experiments and simulations describing similar findings in CA1 pyramidal neurons. We thank D. Attwell, B. Clark, M. Farrant, A. Roth, J. Rothman, A. Silver, S. Wang, and S. Williams for comments on the manuscript. We acknowledge support from The Wellcome Trust, the European Community (M.H.), the Human Frontier Science Program (G.J.S.), and Lucent Technologies (G.M.).

25 September 2000; accepted 26 October 2000

Migration of *Plasmodium* Sporozoites Through Cells Before Infection

Maria M. Mota,¹ Gabriele Pradel,² Jerome P. Vanderberg,² Julius C. R. Hafalla,² Ute Frevert,² Ruth S. Nussenzweig,² Victor Nussenzweig,¹ Ana Rodriguez^{2*}

Intracellular bacteria and parasites typically invade host cells through the formation of an internalization vacuole around the invading pathogen. *Plasmodium* sporozoites, the infective stage of the malaria parasite transmitted by mosquitoes, have an alternative mechanism to enter cells. We observed breaching of the plasma membrane of the host cell followed by rapid repair. This mode of entry did not result in the formation of a vacuole around the sporozoite, and was followed by exit of the parasite from the host cell. Sporozoites traversed the cytosol of several cells before invading a hepatocyte by formation of a parasitophorous vacuole, in which they developed into the next infective stage. Sporozoite migration through several cells in the mammalian host appears to be essential for the completion of the life cycle.

After *Plasmodium* sporozoites are injected into the mammalian host by mosquitoes, hepatocyte infection is the next obligatory step. In time-lapse video microscopy observations, sporozoites appeared to enter and exit hepatocytes rapidly [(Fig. 1 and Web movie 1) (1)] as previously described for macrophages (2). In most cases, hepatocytes survived after parasite entry and exit, but on several occasions cell material was observed leaking into the medium from the site of sporozoite egress, followed by death of the host cell.

To determine whether sporozoites disrupt the hepatocyte plasma membrane while traversing host cells, we used a standard cell wounding and membrane repair assay (3). Wounded cells can be identified by the presence of a cell-impermeant tracer macromolecule within their cytosol, because an open plasma membrane dis-

ruption allows the tracer to enter, after which resealing traps it inside the cell. Dead cells, which do not reseal, are not labeled provided that all exogenous tracer is washed away after membrane disruption. *Plasmodium yoelii* sporozoites, obtained by dissection of infected mosquito salivary glands, were incubated with a mouse hepatoma cell line, Hepa 1-6 (4), in the presence of the cell-impermeant tracer fluorescein isothiocyanate (FITC)-dextran. As a control, Hepa 1-6 cells were incubated with material obtained by dissection of noninfected mosquito salivary glands. After 1 hour, cells were washed to remove all exogenous tracer, then incubated with propidium iodide to detect dead cells. Propidium iodide and dextran-positive cells were found only in cultures incubated with *P. yoelii* sporozoites (Fig. 2A). Endocytosed FITC-dextran was observed as a fine dotted pattern in cell cytosol and was easily distinguished from cytosolic dextran (Fig. 2, A and B). Increasing numbers of Hepa 1-6 cells containing cytosolic dextran were observed up to 1 hour after incubation, remaining constant after this time (Fig. 2C). Sporozoite motility and infectivity are also severely reduced after 1 hour

of incubation. The percentage of dextran-positive cells varied between 10 and 30% in different sporozoite preparations. The percentage of propidium iodide-positive cells reached $\sim 5\%$, but the total number of dead cells is probably higher because cells detach from the substrate soon after they die. Flow cytometric analysis (FACS) showed similar percentages of dextran-positive cells and revealed an increase in the size of dextran-positive cells, as described for other cells that have suffered plasma membrane wounding and repair (5).

Wounding of the plasma membrane results in leakage of cytosolic material into the external medium (6). To test whether sporozoites induce release of cytosol from hepatocytes, we incubated *P. yoelii* sporozoites with Hepa 1-6 cells previously loaded with the cytosolic fluorescent marker Green Cell Tracker. *Plasmodium yoelii* sporozoites induced progressive release of this cytosolic marker into the medium (Fig. 2D). These results indicate that sporozoites induce disruption of the host cell membrane, followed by death or survival of the cell, depending on successful resealing of the plasma membrane.

Sporozoites from different *Plasmodium* species, including the human malarial pathogen *Plasmodium falciparum*, displayed similar capacities to induce wounding and repair in Hepa 1-6 cells. Tachyzoites of another apicomplexan parasite, *Toxoplasma gondii*, also infected Hepa 1-6 cells; however, no dextran- or propidium iodide-positive cells were found in the cultures [Web fig. 1 (1)]. *Plasmodium* sporozoites induced similar levels of wounding in other types of mammalian cells, such as fibroblast and epithelial cell lines [Web fig. 2 (1)].

Sporozoite motility was inhibited by three different mechanisms before incubation with Hepa 1-6 cells to investigate if cell wounding was a result of active penetration of host cells by sporozoites: (i) heat inactivation (7), (ii) incubation with the actin-depolymerizing drug cytochalasin-D (8), and (iii) incubation with a monoclonal antibody (mAb) against *P. yoelii* circumsporozoite protein (anti-CS mAb) (9, 10). All treatments significantly inhibited cell wounding, as measured by a reduction in the

¹Department of Pathology, ²Department of Medical and Molecular Parasitology, New York University School of Medicine, 341 East 25 Street, New York, NY 10010, USA.

*To whom correspondence should be addressed. E-mail: rodria02@popmail.med.nyu.edu

REPORTS

proportion of dextran-positive cells (Fig. 2E) and the release of the cytosolic fluorescent marker from Hepa 1–6 cells. During the process

of gliding motility, sporozoites leave behind trails of surface proteins that can be visualized by staining with anti-CS mAbs (11). Frequently,

these trails were found indicating sporozoite entry into dextran-positive cells (Fig. 2F).

Mardin Darby canine kidney (MDCK) cells form tight junctions and create tightly sealed polarized monolayers when cultured on filters (12). This system was used to verify that sporozoites can traverse an epithelial cell barrier. The continuity of the monolayer and the formation of tight junctions were confirmed by measuring the absence of permeability to 10-kD dextran (13). *Plasmodium yoelii* sporozoites were added onto the MDCK cells in the upper chamber. Any sporozoites that crossed the monolayer could be quantified by counting the numbers of infected Hepa 1–6 cells cultured on cover slips placed underneath the filters in the lower chamber (Table 1). Dextran-positive cells were found in both the MDCK cell monolayer and the underlying Hepa 1–6 cells. This indicates that sporozoite-induced cell wounding is caused by parasites actively traversing cells. When sporozoite motility was inhibited by heat inactivation or by preincubation with anti-CS mAb, cell wounding and Hepa 1–6 cell infection were significantly reduced (Table 1).

To test whether invasion of *Plasmodium* sporozoites by plasma membrane disruption and repair leads to parasites lacking vacuolar membranes within the host cell cytosol, we developed an assay using a label for the sporozoite parasitophorous vacuole. The plasma membranes of Hepa 1–6 cells were labeled with fluorescent agglutinin before incubation with sporozoites; because agglutinin does not bind to *P. yoelii* sporozoites [Web fig. 2 (I)], any agglutinin on an intracellular parasite would indicate that they are surrounded by a parasitophorous vacuole derived from the host cell plasma membrane. Sporozoites surrounded by parasitophorous vacuole membranes were found only inside dextran-negative cells ($n = 5$) (Fig. 3, B and D), whereas sporozoites lacking surrounding vacuolar membranes were found only inside dextran-positive cells ($n = 19$) (Fig. 3, A and C). The majority of dextran-positive cells do not contain sporozoites in their cytosol because parasites rapidly migrate into and out of cells. When *T. gondii* tachyzoites were used in this assay, all intracellular parasites were found to be surrounded by agglutinin-labeled parasitophorous vacuoles [Web fig. 2 (I)]. Electron microscopy studies on Hepa 1–6 cells incubated with *P. yoelii* sporozoites for 1 hour showed sporozoites within parasitophorous vacuoles ($n = 6$) (Fig. 3F) or without ($n = 30$) (Fig. 3E) in the cytosol of Hepa 1–6 cells. Disruption of the host cell plasma membrane was also observed (Fig. 3G). Taken together, these results indicate that sporozoites can enter hepatocytes not only by formation of an internalization vacuole that surrounds sporozoites, but also by disrupting the plasma membrane, leading to the presence of free sporozoites in the cytosol.

Sporozoites were incubated with Hepa 1–6 cells for 1 hour in the presence of fluorescent

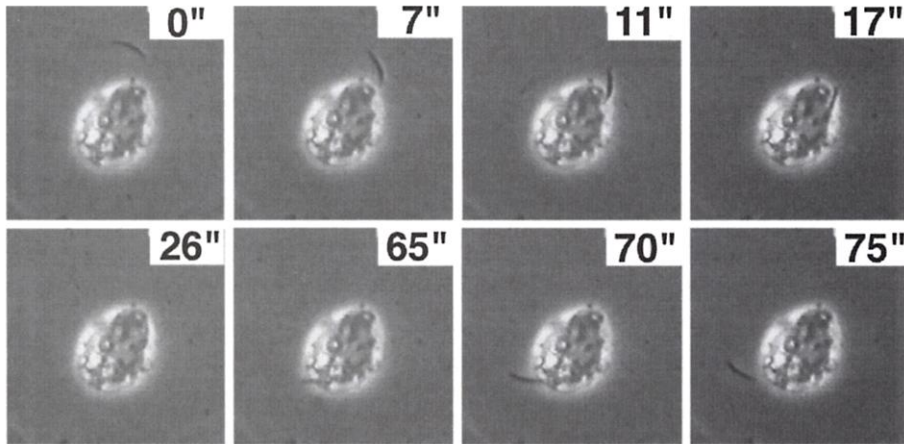
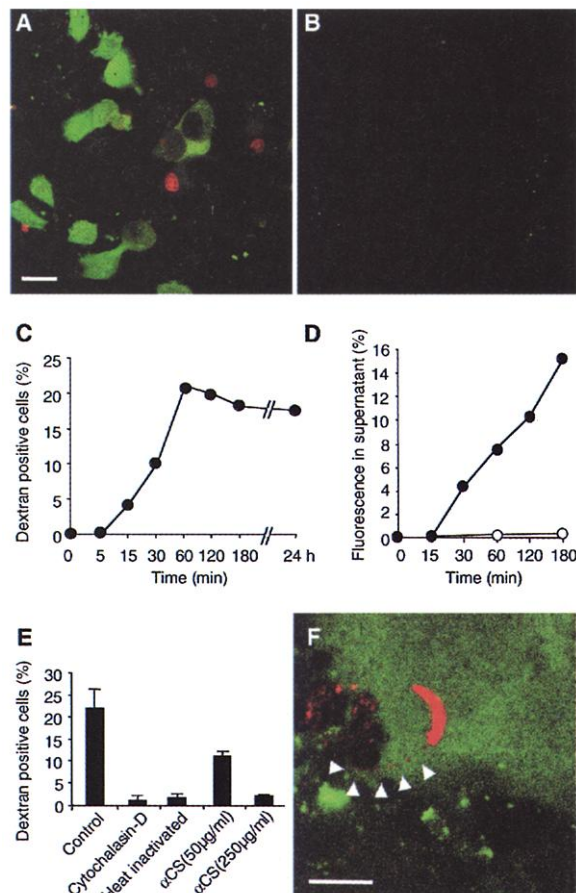


Fig. 1. Sporozoites appear to enter and exit from host cells within 1 min. Time-lapse video images of a *P. berghei* sporozoite entering and exiting a HepG2 hepatocyte. Sequential images are shown, with the time (in seconds) indicated in the upper right corner, covering a total period of 1 min 15 s. This time-lapse movie is available at Web movie 1 (7).

Fig. 2. *Plasmodium* sporozoites induce host cell plasma membrane wounding, followed by repair. (A) *Plasmodium yoelii* sporozoites (10^5) or (B) control material from dissection of the same number of *Anopheles stephensi* mosquito salivary glands were added to monolayers of 2×10^5 Hepa 1–6 cells (in 24-well plates) for 1 hour in the presence of 1 mg/ml FITC-dextran, lysine-fixable, 10,000 MW (Molecular Probes) (green). Cells were washed and incubated with 1 μ g/ml propidium iodide (red) for 5 min before fixation with 4% paraformaldehyde and analysis by confocal microscopy. Bar, 20 μ m. (C) Hepa 1–6 cells (2×10^5) in 24-well plates were incubated with 10^5 *P. yoelii* sporozoites in the presence of FITC-dextran for the times indicated before fixation and quantification of dextran-positive cells (for the 24-hour time point, cells were incubated for 3 hours with dextran, washed, and further incubated until 24 hours in medium). (D) Hepa 1–6 cells (2×10^5) were incubated with the cytosolic marker Green Cell Tracker (Molecular Probes) (10 μ M) for 1 hour and washed before addition of 10^5 *P. yoelii* sporozoites (●) or same number of heat-inactivated sporozoites as control (○).

Supernatants were collected at the times indicated, and Green Cell Tracker was detected by measuring the fluorescence at an excitation wave length of 485 nm and emission wave length of 518 nm. (E) Sporozoite motility was inhibited by heat inactivation (15 min, 56°C), pretreatment of sporozoites with cytochalasin-D (10 μ M for 10 min), or preincubation with anti-CS mAb (50 or 250 μ g/ml for 30 min), before addition to Hepa 1–6 cells in the presence of 1 mg/ml FITC-dextran. (F) *Plasmodium yoelii* sporozoites were incubated for 1 hour with Hepa 1–6 cells in the presence of 1 mg/ml FITC-dextran before fixation and staining with anti-CS mAb (red). The trail, indicated with arrowheads, shows that the sporozoite first moved in circles outside, before entering the Hepa 1–6 cell. Bar, 10 μ m.



REPORTS

dextran, followed by washing and incubation for an additional 24 hours to see if the developing exoerythrocytic form (EEF) of the parasite could be detected. Most of the infected Hepa 1–6 cells containing EEFs were dextran-negative ($95.7 \pm 0.9\%$) (Fig. 4A), indicating that successful development within hepatocytes occurred when sporozoites formed parasitophorous vacuoles. The small percentage of EEFs (4.3%) that developed in dextran-positive cells is probably a result of previous invasion by a migrating sporozoite.

The behavior of individual sporozoites was studied to determine whether or not the population of sporozoites that traverse cells and the population that develops into EEFs were the same. Hepa 1–6 cells were incubated with limiting dilutions of sporozoites in the presence of fluorescent dextran; subsequently, plaques of dextran-positive cells were seen, the number of which increased proportional to the number of sporozoites added in the culture. Each plaque presumably corresponds to a single parasite. After 1 hour of incubation, the average number of dextran-positive cells seen per plaque was counted, and it appeared that each sporozoite traversed an average of four cells in this time. It is likely that sporozoites traverse additional cells that are not able to reseal their membranes, die shortly afterwards, and are not detected. To test if sporozoite migration through cells preceded infection, we washed cultures 1 hour after sporozoites were added and incubated the cultures for an additional 24 hours. The majority of EEFs ($86.4 \pm 3.5\%$) were found next to dextran-positive cells as part of plaques (Fig. 4B), confirming that single sporozoites traversed several cells before pausing to replicate.

A standard assay for detection of cell wounding in animals was used to determine whether the ability of *Plasmodium* sporozoites to traverse through host cells is used by the parasite during infection in vivo (3). The fluorescent dextran tracer was injected intravenously into mice infected with *P. yoelii* sporozoites either by intravenous injection (10^6 sporozoites per mouse) or by the bite of infected mosquitoes. Histological sections of mouse livers analyzed by confocal microscopy revealed a high density of dextran-positive hepatocytes (400 to $900/\text{cm}^2$) in mice infected intravenously. In mice infected by mosquito bite, fewer dextran-positive hepatocytes were observed ($3.3 \pm 1.5/\text{cm}^2$). No dextran-positive cells were found in the livers of mice injected with heat-inactivated sporozoites or with material obtained from dissection of noninfected mosquito salivary glands. Sporozoites were often found close to dextran-positive hepatocytes (Fig. 4C), suggesting that sporozoites traverse several hepatocytes in the liver of the host before infection, as observed in vitro.

Invasion of host cells by bacteria and parasites occurs without disruption of the host cell plasma membrane, and is typically

accompanied by the formation of a membrane vacuole surrounding the infectious agent. Our results show that *Plasmodium*

sporozoites have an alternative mechanism of entry into mammalian cells involving direct penetration of the host cell plasma mem-

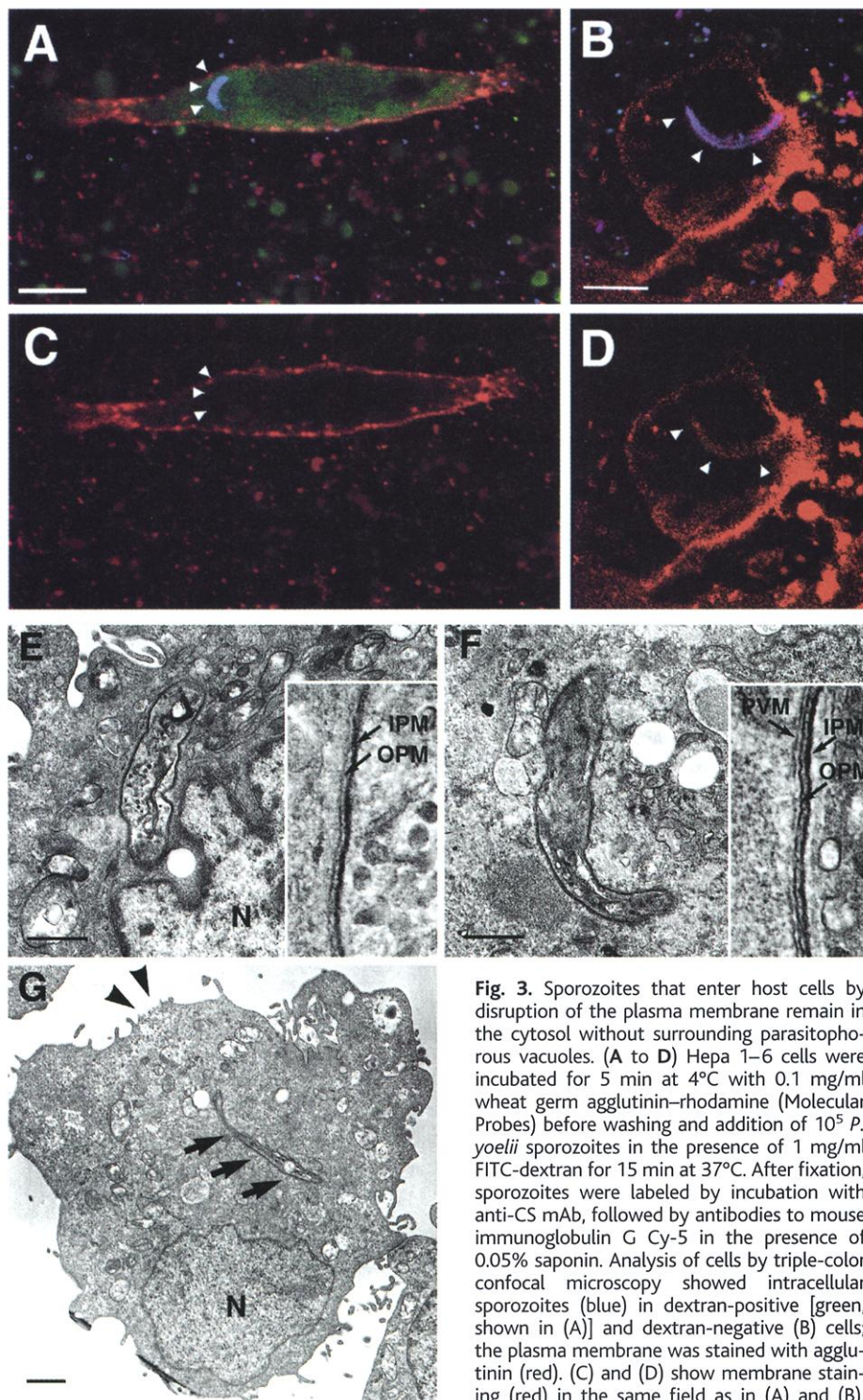


Fig. 3. Sporozoites that enter host cells by disruption of the plasma membrane remain in the cytosol without surrounding parasitophorous vacuoles. (A to D) Hepa 1–6 cells were incubated for 5 min at 4°C with 0.1 mg/ml wheat germ agglutinin–rhodamine (Molecular Probes) before washing and addition of 10^5 *P. yoelii* sporozoites in the presence of 1 mg/ml FITC-dextran for 15 min at 37°C . After fixation, sporozoites were labeled by incubation with anti-CS mAb, followed by antibodies to mouse immunoglobulin G Cy-5 in the presence of 0.05% saponin. Analysis of cells by triple-color confocal microscopy showed intracellular sporozoites (blue) in dextran-positive [green, shown in (A)] and dextran-negative (B) cells; the plasma membrane was stained with agglutinin (red). (C) and (D) show membrane staining (red) in the same field as in (A) and (B), respectively. A parasitophorous vacuole surrounding intracellular sporozoites was observed only in dextran-negative cells (B and D). Bar, 5 μm . (E to G) Hepa 1–6 cells were incubated for 1 hour with sporozoites, trypsinized, and fixed in 4% paraformaldehyde and 0.1% glutaraldehyde, before dehydration in ethanol and Epon embedding (17). Samples were analyzed by electron microscopy. Bar, 1 μm . Insets in (E) and (F) show an enlargement of sporozoite pellicle, constituted by the inner pellicular membrane (IPM) and the outer pellicular membrane (OPM), which are surrounded (F) or not (E) by a parasitophorous vacuole membrane (PVM). (G) Arrows point to a sporozoite free in the cytosol of an Hepa 1–6 cell which shows a disruption in the plasma membrane (arrowheads), probably the site of entry of the sporozoite.

REPORTS

brane. By this means, sporozoites traverse several cells before finally engaging the established cell entry mechanism for the hepatocyte where they develop and replicate (Fig. 4D). Sporozoites from *Plasmodium* spp. and species of the related apicomplexan parasite *Eimeria* have been found frequently without a parasitophorous vacuole in the cytosol of host cells shortly after infection both in vitro and in vivo (14–18). These observations were difficult to explain in the context of apicomplexan infection, because the development of intracellular parasites has always been observed within a well-delimited parasitophorous vacuole (19–22). Our findings provide an explanation for these observations. *Eimeria* and *Toxoplasma* sporozoites (but not tachyzoites) have also been observed

to enter and exit cultured cells (15, 16, 23), suggesting that other apicomplexan parasites may also have the ability to traverse through host cells before infection. Recent studies on ookinetes, a mosquito stage of the malaria parasite, suggest that they too disrupt the plasma membrane of epithelial cells to penetrate the mosquito midgut (24, 25).

The ability of *Plasmodium* sporozoites to traverse mammalian cells raises important questions about the role of this process in the development of malaria infection and the mechanisms used by sporozoites to disrupt the plasma membrane and to move within host cells. Sporozoites may need to traverse several cells to activate signaling pathways necessary for entering and further development in hepatocytes, or to search for specific hepatocytes that

are suitable for infection. In addition, before arriving in the liver, sporozoites need to migrate through cellular barriers in the skin, after inoculation by mosquitoes (26–28), to reach the circulatory system. The ability of sporozoites to traverse host cells is probably essential for this step of the *Plasmodium* life cycle.

References and Notes

- Web movie 1, Web fig. 1, and Web fig. 2 are available at Science Online at www.sciencemag.org/cgi/content/full/291/5501/141/DC1.
- J. P. Vanderberg, S. Chew, M. J. Stewart, *J. Protozool.* **37**, 528 (1990).
- P. L. McNeil, M. F. S. Clarke, K. Miyake, in *Current Protocols in Cell Biology*, I. J. S. Bonifacio, M. Dasso, J. B. Harford, J. Lippincott-Schartz, K. M. Yamada, Eds. (Wiley, New York, 1999), pp. 12.4.1–12.4.15.
- M. M. Mota, A. Rodriguez, *Exp. Parasitol.*, in press.
- K. Miyake, P. L. McNeil, *J. Cell Biol.* **131**, 1737 (1995).
- L. Muthukrishnan, E. Warder, P. L. McNeil, *J. Cell. Physiol.* **148**, 1 (1991).
- G. L. Spitalny, R. Nussenzweig, *Proc. Helminthol. Soc. Wash.* **39**, 506 (1972).
- M. J. Stewart, J. P. Vanderberg, *J. Protozool.* **38**, 411 (1991).
- Y. Charoenvit, M. F. Leef, L. F. Yuan, M. Sedegah, R. L. Beaudoin, *Infect. Immun.* **55**, 604 (1987).
- M. J. Stewart, R. J. Nawrot, S. Schulman, J. P. Vanderberg, *Infect. Immun.* **51**, 859 (1986).
- M. J. Stewart, J. P. Vanderberg, *J. Protozool.* **35**, 389 (1988).
- M. Cereijido, E. S. Robbins, W. J. Dolan, C. A. Rotunno, D. D. Sabatini, *J. Cell Biol.* **77**, 853 (1978).
- S. T. Jiang et al., *Kidney Int.* **56**, 92 (1999).
- M. Aikawa, A. Schwartz, S. Uni, R. Nussenzweig, M. Hollingdale, *Am. J. Trop. Med. Hyg.* **33**, 792 (1984).
- B. Chobotar, H. D. Danforth, R. Entzeroth, *Parasitol. Res.* **79**, 15 (1993).
- H. D. Danforth, R. Entzeroth, B. Chobotar, *Parasitol. Res.* **78**, 570 (1992).
- F. U. Hugel, G. Pradel, U. Frevert, *Mol. Biochem. Parasitol.* **81**, 151 (1996).
- S. C. Shin, J. P. Vanderberg, J. A. Terzakis, *J. Protozool.* **29**, 448 (1982).
- R. Entzeroth, F. R. Mattig, R. Werner-Meier, *Int. J. Parasitol.* **28**, 1015 (1998).
- P. C. Garnham, R. G. Bird, J. R. Baker, R. Killck-Kendrick, *Trans. R. Soc. Trop. Med. Hyg.* **63**, 328 (1969).
- J. F. Meis, J. P. Verhave, P. H. Jap, R. E. Sinden, J. H. Meuwissen, *Nature* **302**, 424 (1983).
- T. Sodeman, B. Schnitzer, T. Durkee, P. Jcontacos, *Science* **170**, 340 (1970).
- C. A. Speer, J. P. Dubey, J. A. Blixt, K. Prokop, *J. Parasitol.* **83**, 565 (1997).
- H. Zieler, J. A. Dvorak, *Proc. Natl. Acad. Sci. U.S.A.* **97**, 11516 (2000).
- Y. S. Han, J. Thompson, F. C. Kafatos, C. Barillas-Mury, *EMBO J.* **19**, 6030 (2000).
- M. F. Boyd, S. F. Kitchen, *Am. J. Trop. Med. Hyg.* **19**, 27 (1939).
- R. B. Griffiths, R. M. Gordon, *Ann. Trop. Med. Parasitol.* **46**, 311 (1952).
- S. Sidjanski, J. P. Vanderberg, *Am. J. Trop. Med. Hyg.* **57**, 426 (1997).
- M. Tsuji, D. Mattei, R. S. Nussenzweig, D. Eichinger, F. Zavala, *Parasitol. Res.* **80**, 16 (1994).
- We thank M. Ronemus and P. Sinnis for critically reviewing the manuscript, M. Starz for help with confocal microscopy, J. Hirst for FACS analysis and sorting, I. Caro and S. Nossair for mosquito dissection, and E. Dy, P. Arriola-Villalobos, and B. Diaz-Ley for technical assistance. The anti-CS mAb (NYS1) was provided by S. Hoffman (Naval Medical Research Center), *P. falciparum* by E. Nardin (NYU School of Medicine), *T. gondii* by D. Roos (University of Pennsylvania), and anti-GRA3 mAb by K. Joiner (Yale University). Supported by the Starr Foundation, Deutscher Akademischer Austauschdienst (G.P.), and American Liver Foundation (A.R.).

Fig. 4. Sporozoites traverse several cells before infection in vitro and in vivo. Hepa 1–6 cells were incubated with 10^5 (A) or 5×10^3 (B) *P. yoelii* sporozoites for 1 hour in the presence of 1 mg/ml FITC-dextran (green). Cells were washed and incubated for another 24 hours before fixation and incubation with anti-CS mAb (red). Cells were analyzed by confocal microscopy. Bar, 20 μ m. (C) BALB/c mice of 6 weeks of age were injected intravenously with 8 mg of FITC-dextran in phosphate-buffered saline (PBS) and 10^6 *P. yoelii* sporozoites, the same amount of heat-inactivated *P. yoelii* sporozoites, or salivary gland material obtained from dissection of an equivalent number of uninfected mosquitoes. After 45 min, mice were anesthetized, followed by liver perfusion with 20 ml of PBS to wash away extracellular FITC-dextran and fixation with 20 ml of 8% paraformaldehyde. Livers were dissected and infiltrated with 30% sucrose in PBS before freezing and sectioning. Histological sections of livers were incubated with anti-CS mAb (red). Bar, 5 μ m. (D) Model of hepatocyte invasion by *Plasmodium* sporozoites.

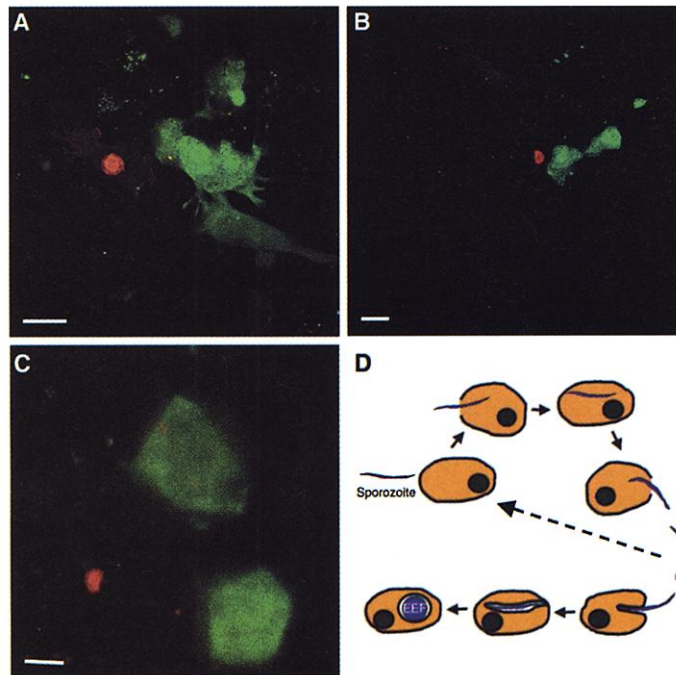


Table 1. Sporozoite motility is required to traverse epithelial monolayers. We cultivated 10^5 MDCK cells in 3- μ m pore diameter Transwell filters (Costar) for 3 days until they formed a continuous monolayer. Cover slips with 3×10^5 Hepa 1–6 cells were placed underneath the filters in the lower chamber. *Plasmodium yoelii* sporozoites (2×10^5), heat-inactivated or preincubated with anti-CS mAb (250 μ g/ml for 30 min), were added in the filter inset. FITC-dextran (1 mg/ml) was also added to the filter inset and lower chamber. MDCK and Hepa 1–6 cells were washed after 2 hours and further incubated for 24 hours before fixation, staining, and quantification of dextran-positive cells and developing parasites with anti-EEFs mAb (29).

Sporozoites	Dextran-positive MDCKs (3×10^5)	Dextran-positive Hepa 1–6 (3×10^5)	EEFs in Hepa 1–6 (3×10^5)
Untreated	1612 \pm 98	652 \pm 51	39 \pm 2.5
Heat-inactivated	151 \pm 56	53 \pm 12	0
+Anti-CS mAb	123 \pm 48	12 \pm 9	0

5 October 2000; accepted 22 November 2000